Paper No: 42

FINITE DIFFERENCE TECHNIQUES AND ROTOR BLADE AEROELASTIC PARTIAL DIFFERENTIAL EQUATIONS: AN EXPLICIT TIME-SPACE FINITE ELEMENT APPROACH FOR P.D.E

Y. K. Yillikci and S. Hanagud
School of Aerospace Engineering
Georgia Institute of Technology
Atlanta, GA 30332, U.S.A

FIFTEENTH EUROPEAN ROTORCRAFT FORUM
September 12-15, 1989, Amsterdam, NETHERLANDS

FINITE DIFFERENCE TECHNIQUES AND ROTOR BLADE AEROELASTIC PARTIAL DIFFERENTIAL EQUATIONS: AN EXPLICIT TIME-SPACE FINITE ELEMENT APPROACH FOR P.D.E.

Y. K. Yillikçi[1] and S. Hanagud[2]
School of Aerospace Engineering,
Georgia Institute of Technology
Atlanta, GA 30332, U.S.A.

Abstract

A conditionally stable explicit finite difference scheme is used to numerically integrate the nonlinear partial differential equations of motion in space and time to obtain the aeroelastic steady-state and transient responses of a hingeless rotor blade. Numerical stability analysis is performed for soft and stiff inplane blades. The effect of different spatial discretizations on blade responses and the convergence of the finite difference scheme are also analyzed. Rotor blade responses are calculated for different blade configurations and results are compared with the results of previous analysis.

LIST OF SYMBOLS

b	rotor blade semichord, l
C_W	helicopter weight coefficient
$\bar{G}\bar{J}$	nondimensional torsional stiffness, $\frac{GJ}{m_{ref}\Omega^2 R^4}$
k_A	radius of gyration of cross section, l
k_m	mass radius of gyration of cross section, $k_m^2 = k_{m_1}^2 + k_{m_2}^2$ l
L_v, L_w	components of lift in lagwise and flapwise directions, fl^{-1}
$\bar{m}$	nondimentional mass per unit lenght
M_ϕ	aerodynamic moment about spanwise axis, f
m	number of spatial mesh points
R	rotor blade radius, l
u, v, w	elastic displacements in spanwise, lagwise and flapwise directions, l
U_P, U_T	velocity components of airfoil in lagwise and flapwise directions with respect to the fluid, lt^{-1}
α_v	rotor disk angle of attack, rad
β_p	precone angle, rad
γ	Lock number
$\theta_0, \theta_{1C}, \theta_{1S}$	pitching control inputs for blade, rad
λ_0	rotor induced uniform inflow, 3.2
Λ_1	nondimensional flapwise stiffness, $\frac{EI_{y'}}{m_{ref}\Omega^2 R^4}$
Λ_2	nondimensional edgewise stiffness, $\frac{EI_{z'}}{m_{ref}\Omega^2 R^4}$
μ	nondimensional forward speed, $\frac{V}{\Omega^2 R}$
$\rho()$	spectral radius of a matrix
σ	solidity, $\frac{bc}{\pi R}$
ϕ	rotation about elastic axis including components bending and torsion, rad
ψ	nondimensional time or azimuth angle $\psi = \Omega t$, rad t
Ω	rotor rotational frequency, $rad\ t^{-1}$
$()^+$	$\frac{\partial}{\partial \bar{x}}$
$()^{++}$	$\frac{\partial^2}{\partial \bar{x}^2}$
$\dot{()}$	$\frac{\partial}{\partial \psi}$
$\ddot{()}$	$\frac{\partial^2}{\partial \psi^2}$

[1] Post Doctoral Fellow
[2] Professor

INTRODUCTION

In contrast to a fixed wing aircraft, both lift and thrust of a helicopter are obtained from its rotor system. A significant part of the control inputs is also applied through the rotor system. The stability analysis and response calculations of rotor blades constitute a significant part of the dynamical and structural analysis of a complete helicopter. The analysis of the rotor blade system is inherently coupled with the unsteady aerodynamics of the translating, rotating, pitching and deflecting rotor blade.

As result of continuing efforts to develop rotor blade configurations with better maintanence and performance characteristics, hingeless and bearingless rotor blades have been developed. With a hingeless blade, flap and lag hinges are eliminated. A bearingless rotor is a special case of the hingeless rotor where even the pitch bearing is eliminated. The bearingless configuration consists of a flexbeam with a wrap-around type of torque tube. The pitch control is applied through this torsionally stiff torque tube. The scope of this study is concerned with the application of finite difference method to solve the rotor blade aeroelastic equations of a hingeless rotor systems. Before discussing the scope of the study, developments in the field of rotor blade aeroelasticity are briefly reviewed.

Numerical Methods for Response Calculations

Usually, as a first step in the solution of rotor blade equations, the spatial dependency is eliminated either by the use of global Galerkin methods [1,2,3] or by the use of finite element methods [4,5,6,7,9]. For aeroelastic stability analysis, nonlinear rotor blade equations are linearized about an appropriate equilibrium or a steady-state. Stability boundaries are then obtained by an eigen analysis. A very detailed survey on formulations of rotor blade aeroelasticity problems is given by Friedmann [8]. After the spatial dependency is eliminated, equations of motion of rotor blades in forward flight are mathematically represented by a system of coupled ordinary differential equations with periodic coefficients in time. These equations can be either linear or nonlinear.

Straub and Friedmann [4] have solved nonlinear rotor blade equations by a quasilinearization procedure for flap-lag motions in forward flight. At each iteration step, nonlinear equations are linearized by expanding the nonlinear equations in a Taylor's series about the previous linearized solution. A similar quasilinear iterative method has been used to obtain nonlinear response with flap-lag-torsion motions in forward flight by Friedmann and Kottapalli [19]. A different type of quasilinearization procedure introduced by Dugundji and Wendell [10], has been used by Panda and Chopra [9] for the solution of nonlinear rotor blade equations with flap-lag-torsion motions. Another approach to response calculations is due to Jonnalagadda and Pierce [1] where a periodic shooting technique, utilizing the Floquet transition matrix through an iterative scheme, has been used. Karunamoorthy and Peters [3] have used a Galerkin time-history solution method to obtain numerical results for forward flight.

Recently, Borri [11] has introduced a time finite element approximation method to calculate the steady response of a fully articulated rotor blade. For response calculations of composite rotor blades, Panda and Chopra [12] have introduced a different type of time finite element method by using Hamilton's principle in weak form. Izadpanah [13] has used a p-version of time finite element method to obtain the flapping response of an articulated rotor blade. In this paper different aspects of finite elements in time methods are discussed in detail and a general bilinear formulation with a proof of convergence has been presented. This bilinear formulation is based on a form of the Hamilton's varying action principle.

As an example of transient response studies, Bir and Chopra [6,7] have investigated the gust response of a coupled hingeless rotor and fuselage system in hover and forward flight conditions. Flap bending, lag bending and torsion deflections of each rotor blade were considered. Governing equations of rotor blades were discretized by a finite element method in space introduced by Sivaneri and Chopra [5]. The fuselage was permitted to have three translational (vertical, longitudinal and lateral) and two rotational (pitch and roll) degrees of freedom. Equations of the overall system were combined by use of the multiblade coordinate system. These equations were linearized with respect to the vehicle propusive trim state and blade steady-state deflected position. The set of linearized coupled ordinary differential equations were then integrated by a fourth-order Runge-Kutta routine to calculate transient response of a fuselage-rotor system that was subjected to gust loads.

Present Study: Numerical Methods

Transient and steady state responeses of rotor blades are usually obtained by first eliminating the spatial dependency. Nonlinear ordinary differential equations in time are then integrated by using linearizations at some stage of the analysis. The objective of this paper is to use an explicit finite difference procedure to numerically integrate the nonlinear partial differential equations of motion in space and time and obtain the aeroelastic response of the rotor blade. This can be considered as a finite element method in time and space. Finite difference methods, on which the method is based, have been developed and used extensively in the field computational fluid mechanics [15,20,21,22,23] Infact, present study can be described as a different type finite element method based on P.D.E rather than the energy method.

Finite difference methods are approximate in the sense that the derivatives at a point are approximated by differences over a small interval. In this paper, a direct integration of nonlinear partial differential equations of rotor blades will not introduce any additional approximations other than the finite difference approximation for the derivatives.

As is discussed in subsequent sections, unlike finite element methods, large inversion of matrices are not required when an explicit finite difference procedure is used to integrate hyperbolic partial differential equations. Simply, variables at a time $(t + \Delta t)$ are calculated from their values at time t. Errors are of the order of $\Delta t, \Delta x$ and Δx^2 depending on the use of a first order or a second order difference scheme. Theorems on consistency assure that the differential equation solutions are achieved as spatial mesh lenght Δx and time interval Δt tend to zero. Stability ia assured by satisfying an appropriate relationship between the spatial mesh lenght Δx and time interval Δt. Only additional time required is in the calculation of stability requirement at each stage. Convergence is assured as Δt increases on the basis of consistency and stability.

In an earlier paper, authors have used finite difference methods to flap-lag solutions of a hingeless blade with success. In this paper complete flap-lag-torsion equations have been solved and compared with results of Taylor [18] where Galerkin method has been used for spatial discretization and time dependency has been eliminated by the use of harmonic balance technique.

FORMULATION

For purposes of numerical integration by the proposed approach which is based on explicit finite difference methods, it is convenient to express the coupled nonlinear partial differential equations of rotor blade system in terms of first order time and second order space derivatives. This reduction is performed by introducing the following variables.

$$\begin{aligned} v_t &= \dot{\bar{v}} \\ w_t &= \dot{\bar{w}} \\ \phi_t &= \dot{\bar{\phi}} \end{aligned} \tag{1}$$

and

$$\begin{aligned} m_v &= \bar{v}^{++} \\ m_w &= \bar{w}^{++} \end{aligned} \tag{2}$$

$$\dot{m}_v = v_t^{++} \tag{3}$$

$$\dot{m}_w = w_t^{++} \tag{4}$$

where $()^{\cdot}$ and $()^{+}$ are the partial derivatives with respect to nondimensional time variable, ψ, azimuth angle, and nondimentional spanwise location variable, $\bar{x}$, respectively. In terms of these variables, rotor blade partial differential equations and the trailing terms can be written in a matrix form as follows,

$$\begin{aligned} \dot{\mathbf{u}}_t = {} & \bar{\mathbf{A}}(\mathbf{u},\psi)\mathbf{u}_m^{++} + \bar{\mathbf{B}}(\mathbf{u},\psi)\mathbf{u}_d^{++} + \bar{\mathbf{C}}(\mathbf{u},\psi)\mathbf{u}_d^{+} + \bar{\mathbf{D}}\mathbf{u}_t \\ & + \bar{\mathbf{E}}(\mathbf{u},\psi)\mathbf{u}_m + \bar{\mathbf{F}}(\psi)\mathbf{u}_d + \bar{\mathbf{g}}(\mathbf{u},\psi) \end{aligned} \tag{5}$$

$$\dot{\mathbf{u}}_m = \mathbf{I}_{23}\mathbf{u}_t^{++} \tag{6}$$

$$\dot{\mathbf{u}}_d = \mathbf{I}_{33}\mathbf{u}_t \tag{7}$$

where $\mathbf{u}_d$ and $\mathbf{u}_t$ are displacement and velocity vectors respectively. The quantity $\mathbf{u}_m$ is vector defined in the following set of equations.

$$\mathbf{u}_t = \left\{ \begin{array}{c} v_t \\ w_t \\ \phi_t \end{array} \right\} \quad \mathbf{u}_m = \left\{ \begin{array}{c} m_v \\ m_w \end{array} \right\}, \quad \mathbf{u}_d = \left\{ \begin{array}{c} \bar{v} \\ \bar{w} \\ \bar{\phi} \end{array} \right\} \tag{8}$$

The vectors $\mathbf{u}_d$, $\mathbf{u}_t$ and $\mathbf{u}_m$ can be combined into a vector $\mathbf{u}$ as

$$\mathbf{u} = \left\{ \begin{array}{c} \mathbf{u}_t \\ \mathbf{u}_m \\ \mathbf{u}_d \end{array} \right\} \tag{9}$$

The matrices $\bar{\mathbf{A}}, \bar{\mathbf{B}}, \ldots, \bar{\mathbf{F}}$ and $\bar{\mathbf{g}}$ are then defined as follows.

$$\bar{\mathbf{A}}(\mathbf{u}, \psi) = -\frac{1}{\bar{m}} \begin{bmatrix} B_{22} - B_{23}\phi & \frac{1}{2}B_{23} + B_{32}\phi \\ \frac{1}{2}B_{23} + B_{32}\phi & B_{33} + B_{23}\phi \\ 0 & 0 \end{bmatrix} \tag{10}$$

$$\bar{\mathbf{B}}(\mathbf{u}, \psi) = -\frac{1}{\bar{m}} \begin{bmatrix} 0 & 0 & B_{32}m_w - B_{23}m_v \\ 0 & 0 & B_{32}m_v + B_{23}m_w \\ 0 & 0 & -\frac{1}{\bar{k}_m^2}GJ - \frac{\bar{k}_A^2}{\bar{k}_m^2}\int_{\bar{x}}^1 \bar{m}(\bar{\xi} + 2v_t)d\bar{\xi} \end{bmatrix} \tag{11}$$

$$\bar{\mathbf{C}}(\mathbf{u}, \psi) = -\frac{1}{\bar{m}} \begin{bmatrix} \bar{m}(\bar{x} + 2v_t) & 0 & -2B_{23}m_v^+ + 2B_{32}m_w^+ \\ 0 & \bar{m}(\bar{x} + 2v_t) & 2B_{23}m_w^+ + 2B_{32}m_v^+ \\ 0 & 0 & \frac{\bar{k}_A^2}{\bar{k}_m^2}\bar{m}(\bar{x} + 2v_t) \end{bmatrix} \tag{12}$$

$$\bar{\mathbf{D}} = -\frac{1}{\bar{m}} \begin{bmatrix} 0 & -2\beta_{pc}\bar{m} & 0 \\ 2\beta_{pc}\bar{m} & 0 & 0 \\ 0 & 0 & 0 \end{bmatrix} \tag{13}$$

$$\bar{\mathbf{E}}(\mathbf{u}, \psi) = -\frac{1}{\bar{m}} \begin{bmatrix} -\int_{\bar{x}}^1 \bar{m}(\bar{\xi} + 2v_t)d\bar{\xi} & 0 \\ 0 & -\int_{\bar{x}}^1 \bar{m}(\bar{\xi} + 2v_t)d\bar{\xi} \\ -\frac{1}{2\bar{k}_m^2}B_{23}m_v & \frac{1}{\bar{k}_m^2}(\frac{1}{2}B_{23}m_w + B_{32}m_v) \end{bmatrix} \tag{14}$$

$$\bar{\mathbf{F}}(\mathbf{u}, \psi) = -\frac{1}{\bar{m}} \begin{bmatrix} -\bar{m} & 0 & 0 \\ 0 & 0 & 0 \\ 0 & 0 & \frac{\bar{m}}{\bar{k}_m^2}\cos 2\theta(\bar{k}_{m_2}^2 - \bar{k}_{m_1}^2) \end{bmatrix} \tag{15}$$

$$\bar{\mathbf{g}}(\mathbf{u}, \psi) = -\frac{1}{\bar{m}} \left\{ \begin{array}{c} -2\bar{m}\int_0^{\bar{x}}(v_t^+\bar{v}^+ + w_t^+\bar{w}^+)d\bar{\xi} + \left[2\bar{m}\,\dot{\bar{\theta}}\,(\bar{k}_{m_2}^2 - \bar{k}_{m_1}^2)\sin\theta\cos\theta\right]^+ - L_v \\ \bar{m}\bar{x}\beta_{pc} + \left[2\bar{m}\,\dot{\bar{\theta}}\,(\bar{k}_{m_2}^2\sin^2\theta + \bar{k}_{m_1}^2\cos^2\theta)\right]^+ - L_w \\ \frac{1}{\bar{k}_m^2}\left[\bar{m}(\bar{k}_{m_2}^2 - \bar{k}_{m_1}^2)\cos\theta\sin\theta + \bar{m}\bar{k}_m^2\,\ddot{\bar{\theta}} - M_\phi\right] \end{array} \right\} \tag{16}$$

where

$$\begin{aligned} B_{22} &= \Lambda_2\cos^2\theta + \Lambda_1\sin^2\theta \\ B_{23} &= (\Lambda_2 - \Lambda_1)\sin 2\theta \\ B_{32} &= (\Lambda_2 - \Lambda_1)\cos 2\theta \\ B_{33} &= \Lambda_2\sin^2\theta + \Lambda_1\cos^2\theta \end{aligned}$$

The boundary conditions at $\bar{x} = 0$

$$\mathbf{q}_d = 0, \quad \bar{v}^+ = 0, \quad \bar{w}^+ = 0 \tag{17}$$

Besides, the boundary conditions at $\bar{x} = 1$ are $\phi^+ = 0$ at $\bar{x} = 1$ and

$$\begin{aligned} \mathbf{A}_{BC_m} \mathbf{q}_{m_m} &= 0 \\ \mathbf{A}_{BC_m} \mathbf{q}^+_{m_m} &= -\left\{ \begin{array}{c} 2\bar{m}\,\dot{\theta}\,(\bar{k}^2_{m_1} - \bar{k}^2_{m_2}) \sin\theta\cos\theta \\ 2\bar{m}\,\dot{\theta}\,(\bar{k}^2_{m_2}\sin^2\theta + \bar{k}^2_{m_1}\cos^2\theta) \end{array} \right\} = \mathbf{k}_I \end{aligned} \tag{18}$$

where matrix $\mathbf{A}_{BC_m}$ is

$$\mathbf{A}_{BC_m} = \left[\begin{array}{cc} B_{22} - \phi_m B_{23} & \frac{1}{2}B_{23} + \phi_m B_{32} \\ \frac{1}{2}B_{23} + \phi_m B_{32} & B_{33} + \phi_m B_{23} \end{array} \right] \tag{19}$$

and in equation (18) $\mathbf{I}_{2,3}$, is defined as

$$\mathbf{I}_{2,3} = \left[\begin{array}{ccc} 1 & 0 & 0 \\ 0 & 1 & 0 \end{array} \right]$$

and $\mathbf{I}_{33}$ is a 3×3 identity matrix.

An Explicit Time Finite Element Approach

Finite difference approximations for rotor blade equations can be formulated in different ways. For time derivatives, the exact solutions of the rotor blade partial differential equations (5-7) $\mathbf{u}^{j+1}_{t_i}$ the node point $(\bar{x}_i, \psi_j + \Delta\psi)$ can be expanded in Taylor series as

$$\mathbf{u}^{j+1}_{t_i} = \mathbf{u}^j_{t_i} + \Delta\psi \mathbf{u}^{j^*}_{t_i} + \frac{1}{2}\Delta\psi^2 \mathbf{u}^{j^{**}}_{t_i} + O(\Delta\psi^3) \tag{20}$$

Vectors $\mathbf{q}^j_{t_i}, \mathbf{q}^j_{m_i}$ and $\mathbf{q}^j_{d_i}$ are defined as approximations for $\mathbf{u}_t, \mathbf{u}_m$ and $\mathbf{u}_d$ at mesh point $(\bar{x}_i, \psi_{j+1})$ when only terms of the order of $\delta\psi$ are retained. Then, they can be combined into a vector $\mathbf{q}^j_i$ as

$$\mathbf{q}^j_i = \left\{ \begin{array}{c} \mathbf{q}^j_{t_i} \\ \mathbf{q}^j_{m_i} \\ \mathbf{q}^j_{d_i} \end{array} \right\} \tag{21}$$

With these approximations for time derivatives, a conditionally stable, explicit scheme can be introduced by using different azimuthal level substitution into equations(5-7). This scheme can be written as, at $(i, j+1)^{th}$ mesh position in a matrix form as

$$\begin{aligned} \mathbf{q}^{j+1}_{t_i} &= \mathbf{q}^j_{t_i} + \Delta\psi \left\{ \bar{\mathbf{A}}^j_i \delta^2 \mathbf{q}^j_{m_i} + \bar{\mathbf{B}}^j_i \delta^2 \mathbf{q}^j_{d_i} + \bar{\mathbf{C}}^j_i \delta \mathbf{q}^j_{d_i} + \bar{\mathbf{D}}^j_i \mathbf{q}^j_{t_i} + \bar{\mathbf{E}}^j_i \mathbf{q}^j_{m_i} \right. \\ &\quad \left. + \bar{\mathbf{F}}^j_i \mathbf{q}^j_{d_i} + \bar{\mathbf{g}}^j_i \right\} + O(\Delta\psi^2) \end{aligned} \tag{22}$$

$$\mathbf{q}^{j+1}_{m_i} = \mathbf{q}^j_{m_i} + \Delta\psi \mathbf{I}_{23} \delta^2 \mathbf{q}^{j+1}_{t_i} + O(\Delta\psi^2) \tag{23}$$

$$\mathbf{q}^{j+1}_{d_i} = \mathbf{q}^j_{d_i} + \Delta\psi \mathbf{I}_{33} \mathbf{q}^{j+1}_{t_i} + O(\Delta\psi^2) \tag{24}$$

In these equations (22-24) δ and δ^2 are first and second order approximations tor first and second spatial derivatives respectively. In order to obtain a finite difference approximations to spatial derivatives the region to be examined is covered by a rectilinear grid with sides parallel to the x-axis and ψ-axis, with $\Delta\psi$ being the grid spacing in the ψ direction. The x-axis is divided into unequal grids with lines paralell to the ψ-axis with coordiates $x = x_i, i = 0, 2, \ldots, m$ where $x_0 = 0$ and $x_n = 1$ as seen in Figure 1. This forms a grid rectangular time finite elements in time and space. The mesh points (x, ψ) are given by $x = x_i$, $\psi = N\Delta\psi$, where N is number of time intervals and $x_0 = 0$, $m = 0$ is the origin.

In general the finite difference approximation for the p-th spatial derivative of the variable $u(x)$ at point x_i can be expressed as the sum of weighted discretized values,

$$u^{(p)}(x_i) = \sum_{k=-N}^{k=M} \alpha_k u(x_{i+k}). \tag{25}$$

Approximations to the first and second spatial derivatives can be written respectively as:

$$\frac{\partial u(x_i)}{\partial x} = \alpha_{-1} u(x_{i-1}) + \alpha_0 u(x_i) + \alpha_1 u(x_{i+1}) + O(\Delta x^2) \tag{26}$$

$$\frac{\partial^2 u(x_i)}{\partial x^2} = \beta_{-1} u(x_{i-1}) + \beta_0 u(x_i) + \beta_1 u(x_i) + O(\Delta x^2) \tag{27}$$

where

$$\alpha_{-1} = \frac{-\Delta x_{i+1}}{\Delta x_i(\Delta x_{i+1} + \Delta x_i)}, \quad \alpha_0 = \frac{1}{\Delta x_i} - \frac{1}{\Delta x_{i+1}}, \quad \alpha_1 = \frac{\Delta x_i}{\Delta x_{i+1}(\Delta x_{i+1} + \Delta x_i)} \tag{28}$$

$$\beta_{-1} = \frac{2}{\Delta x_i(\Delta x_{i+1} + \Delta x_i)}, \quad \beta_0 = \frac{-2}{\Delta x_i \Delta x_{i+1}}, \quad \beta_1 = \frac{2}{\Delta x_{i+1}(\Delta x_{i+1} + \Delta x_i)} \tag{29}$$

Where, $\Delta x_i = x_i - x_{i-1}$ and $\Delta x_{i+1} = x_{i+1} - x_i$

The currently calculated velocity vectors $\mathbf{q}_{t_i}^{j+1}$ are substituted into equations (23-24) to calculate defined variables $\mathbf{q}_{m_i}^{j+1}$. As explained later, this procedure makes the overall solution of the set of finite difference equations stable. The equation (24) depend on velocity vector $\mathbf{q}_{d_i}^{j+1}$ and it has been observed that averaging the velocitites vector $\mathbf{q}_{t_i}^{j+1}$ and $\mathbf{q}_{t_i}^{j}$ to calculate displacements has a destabilizing effect on the general solution of the numerical scheme. Therefore, displacements are calculated from equation (24) without averaging th without averaging the velocities. Second order accuracy is obtained for spatial derivatives by central differencing. The accuracy of displacements, velocities and are defined variables are still first order in time.

To complete the formulation of the problem, the trailing terms are also approximated by finite differences. The boundary conditions at $x = 0$ can be rewritten as

$$\mathbf{q}_{t_0} = 0, \quad \mathbf{q}_{d_0} = 0, \quad \mathbf{q}_{m_0} = \frac{2}{\Delta x^2} \mathbf{I}_{23} \mathbf{q}_{d_1} \tag{30}$$

The first spatial derivative of $\mathbf{q}_m$ at $\bar{x} = 1$ can be approximated as third spatial derivative of nodal displacement vector $\mathbf{q}_d$ as

$$\begin{aligned} \mathbf{q}_{m_m}^{+} &= \mathbf{A}_{BC}^{-1} \mathbf{k}_I = \bar{\mathbf{q}}_{d_m}^{+++} \\ \bar{\mathbf{q}}_{d_m}^{+++} &\approx \mathbf{I}_{23}(h_{-2}\mathbf{q}_{d_{m-2}} + h_{-1}\mathbf{q}_{d_{m-1}} + h_0 \mathbf{q}_{d_m} + h_1 \mathbf{q}_{d_{m+1}}) \end{aligned} \tag{31}$$

where

$$\bar{\mathbf{q}}_{d_m} = \mathbf{I}_{23} \mathbf{q}_{d_m} \tag{32}$$

Coefficients h_{-2}, h_{-1}, h_0 and h_1 are obtained for equal mesh sizes as

$$h_{-2} = \frac{-1}{\Delta \bar{x}^3}, h_{-1} = \frac{3}{\Delta \bar{x}^3}, h_0 = \frac{-3}{\Delta \bar{x}^3}, h_1 = \frac{1}{\Delta \bar{x}^3},$$

The variable, $\mathbf{q}_{m_m}$ can be also approximated as

$$\mathbf{q}_{m_m} = \mathbf{q}_{d_m}^{++} \approx \beta_{-1} \bar{\mathbf{q}}_{d_{m-1}} + \beta_0 \bar{\mathbf{q}}_{d_m} + \beta_1 \bar{\mathbf{q}}_{d_{m+1}} = 0 \tag{33}$$

Equations (32) and (33) introduce a fictitious node $m + 1$ which does not have any physical meaning but is needed to approximate the second and third order spatial derivatives at $\bar{x}$.

Finally the complete boundary conditions can now be written for equal element size $\Delta\bar{x}$ as

$$\begin{aligned} \mathbf{q}_{m_m} &= 0 \\ \bar{\mathbf{q}}_{d_m} &= 2\bar{\mathbf{q}}_{d_{m-1}} - \bar{\mathbf{q}}_{d_{m-2}} + \Delta\bar{x}^3 \mathbf{A}_{BC}^{-1} \mathbf{k}_I \\ \phi_m &= \frac{4}{3}\phi_{m-1} - \frac{1}{3}\phi_{m-2} \\ \mathbf{q}_{t_m}^{n+1} &= \frac{\mathbf{q}_{d_m}^{n+1} - \mathbf{q}_{d_m}^{n}}{\Delta\bar{x}} \end{aligned} \tag{34}$$

Approximations for all mesh points can be written globally by using equations (22-24) and combined with boundary conditions given by equations (30) and (34) as

$$\hat{\mathbf{B}}^G \mathbf{q}^{G^{j+1}} = \hat{\mathbf{A}}^{G^j}(\mathbf{q}^{G^j}, \psi)\mathbf{q}^{G^j}(\psi) + \hat{\mathbf{g}}^j(\mathbf{q}^{G^j}, \psi). \tag{35}$$

By multiplying both sides of above equation by $\mathbf{B}^{G^{-1}}$ one can write

$$\mathbf{q}^{G^{j+1}} = \hat{\mathbf{B}}^{G^{-1}} \hat{\mathbf{A}}^{G^j}(\mathbf{q}^{G^j}, \psi)\ \mathbf{q}^{G^j} + \hat{\mathbf{B}}^{G^{-1}} \hat{\mathbf{g}}^j(\mathbf{q}^{G^j}, \psi)$$

or

$$\mathbf{q}^{G^{j+1}} = \check{\mathbf{A}}^{G^j}(\mathbf{q}^{G^j}, \psi)\mathbf{q}^{G^j} + \check{\mathbf{g}}^j(\mathbf{q}^{G^j}, \psi) \tag{36}$$

where

$$\begin{aligned} \check{\mathbf{A}}^{G^j} &= \hat{\mathbf{B}}^{G^{-1}} \hat{\mathbf{A}}^{G^j} \\ \check{\mathbf{g}}^j &= \hat{\mathbf{B}}^{G^{-1}} \hat{\mathbf{g}}^j \end{aligned}$$

Equation (36) can be called the explicit time-space finite element method or explicit finite difference method. The vector of spanwise global nodal vectors, $\hat{\mathbf{q}}$ and column vector of known constants at j^{th} azimuthal step, $\hat{\mathbf{g}}^G$ are written as,

$$\mathbf{q}^G(\psi) = \begin{Bmatrix} \mathbf{q}_1 \\ \mathbf{q}_2 \\ \vdots \\ \mathbf{q}_{m-2} \\ \mathbf{q}_{m-1} \end{Bmatrix}, \qquad \hat{\mathbf{g}}^G = \Delta\psi \begin{Bmatrix} \mathbf{g}_1 \\ \mathbf{g}_2 \\ \vdots \\ \mathbf{g}_{m-2} \\ \mathbf{g}_{m-1} \end{Bmatrix} \tag{37}$$

The spanwise global matrices $\mathbf{A}^{G^j}$ and $\mathbf{B}^{G^j}$ are constructed in terms of the submatrices $\mathbf{A}_{1,2}, \mathbf{A}_{1,3}, \ldots, \mathbf{B}_{m-1,2}$ as

$$\hat{\mathbf{A}}^{G^j} = \begin{bmatrix} \mathbf{A}_{1,2} & \mathbf{A}_{1,3} & & & & & \\ \mathbf{A}_{2,1} & \mathbf{A}_{2,2} & \mathbf{A}_{2,3} & & & & \\ & & & \ddots & & & \\ & & & & \mathbf{A}_{m-2,1} & \mathbf{A}_{m-2,2} & \mathbf{A}_{m-2,3} \\ & & & & & \mathbf{A}_{m-1,1} & \mathbf{A}_{m-1,2} \end{bmatrix} \tag{38}$$

$$\hat{\mathbf{B}}^G = \begin{bmatrix} \mathbf{B}_{1,2} & \mathbf{B}_{1,3} & & & & & \\ \mathbf{B}_{2,1} & \mathbf{B}_{2,2} & \mathbf{B}_{2,3} & & & & \\ & & & \ddots & & & \\ & & & & \mathbf{B}_{m-2,1} & \mathbf{B}_{m-2,2} & \mathbf{B}_{m-2,3} \\ & & & & & \mathbf{B}_{m-1,1} & \mathbf{B}_{m-1,2} \end{bmatrix} \tag{39}$$

Submatrices $\mathbf{A}_{i,1}, \ldots, \mathbf{B}_{i,3}$ and column vector $\mathbf{g}_i$ are written in terms of submatrices $\bar{\mathbf{A}}_i, \bar{\mathbf{B}}_i, \ldots, \bar{\mathbf{D}}_i$ where first and second spatial derivatives are replaced by first and second central differences given by equations (26) and (37).

$$\mathbf{A}_{i,1} = \begin{bmatrix} 0 & \Delta\psi\beta_{-1}\bar{\mathbf{A}}_i & \Delta\psi(\beta_{-1}\bar{\mathbf{B}}_i + \alpha_{-1}\bar{\mathbf{C}}_i) \\ 0 & 0 & 0 \\ 0 & 0 & 0 \end{bmatrix} \tag{40}$$

$$\mathbf{A}_{i,2} = \begin{bmatrix} \Delta\psi\bar{\mathbf{D}}_i + \mathbf{I}_{3,3} & \Delta\psi\left(\beta_0\bar{\mathbf{A}}_i + \bar{\mathbf{E}}_i\right) & \Delta\psi(\beta_0\bar{\mathbf{B}}_i + \alpha_0\bar{\mathbf{C}}_i + \bar{\mathbf{F}}_i) \\ 0 & \mathbf{I}_{2,3} & 0 \\ 0 & 0 & \mathbf{I}_{3,3} \end{bmatrix} \tag{41}$$

$$\mathbf{A}_{i,3} = \begin{bmatrix} 0 & \Delta\psi\beta_1\bar{\mathbf{A}}_i & \Delta\psi(\beta_1\bar{\mathbf{B}}_i + \alpha_1\bar{\mathbf{C}}_i) \\ 0 & 0 & 0 \\ 0 & 0 & 0 \end{bmatrix} \tag{42}$$

$$\mathbf{B}_{i,1} = \begin{bmatrix} 0 & 0 & 0 \\ -\Delta\psi\beta_{-1}\mathbf{I}_{2,3} & 0 & 0 \\ 0 & 0 & 0 \end{bmatrix} \tag{43}$$

$$\mathbf{B}_{i,2} = \begin{bmatrix} \mathbf{I}_{3,3} & 0 & 0 \\ -\Delta\psi\beta_0\mathbf{I}_{2,3} & \mathbf{I}_{2,2} & 0 \\ -\Delta\psi\mathbf{I}_{3,3} & 0 & \mathbf{I}_{3,3} \end{bmatrix} \tag{44}$$

$$\mathbf{B}_{i,3} = \begin{bmatrix} 0 & 0 & 0 \\ -\Delta\psi\beta_1\mathbf{I}_{2,3} & 0 & 0 \\ 0 & 0 & 0 \end{bmatrix} \tag{45}$$

Matrix $\hat{\mathbf{A}}(\mathbf{q}, \psi)$ is nonlinear and is function of the azimuthal step. On the other hand, matrix $\mathbf{B}^G$ is linear and is a function of spatial mesh sixe. The values of $\mathbf{B}^G$ needs to be calculated once for a given $\Delta\bar{x}$, spatial discritizetion. The boundary conditions are introduced to the finite difference scheme through submatrices $\mathbf{A}_{1,2}, \mathbf{A}_{m-1,1}, \mathbf{A}_{m-2,2}$, and $\mathbf{B}_{1,2}, \mathbf{B}_{m-1,1}, \mathbf{B}_{m-2,2}$ and are written as follows

$$\mathbf{A}_{1,2} = \begin{bmatrix} \Delta\psi\mathbf{D}_1 + \mathbf{I}_{3,3} & \Delta\psi\left(\beta_0\mathbf{A}_1 + \mathbf{E}_1\right) & \Delta\psi(\beta_{-1}\frac{2}{\Delta\bar{x}_1}\mathbf{I}_{2,3}\mathbf{A}_1 + \beta_0\mathbf{B}_1 \\ & & +\alpha_0\mathbf{C}_1 + \mathbf{F}_1) \\ 0 & \mathbf{I}_{2,3} & 0 \\ 0 & 0 & \mathbf{I}_{3,3} \end{bmatrix} \tag{46}$$

$$\mathbf{A}_{m-1,1} = \begin{bmatrix} 0 & \Delta\psi\beta_{-1}\mathbf{A}_{m-1} & \Delta\psi[(\beta_{-1} + \beta_1\mathbf{Q}_2)\mathbf{B}_{m-1} \\ & & (\alpha_{-1} + \alpha_1\mathbf{Q}_2)\mathbf{C}_{m-1}] \\ 0 & 0 & 0 \\ \\ 0 & 0 & 0 \end{bmatrix} \tag{47}$$

$$\mathbf{A}_{m-2,2} = \begin{bmatrix} \Delta\psi\mathbf{D}_{m-1} + \mathbf{I} & \Delta\psi\left[\beta_0\mathbf{A}_{m-1} + \bar{\mathbf{E}}_i\right] & \Delta\psi\left[(\beta_0 + \beta_1\mathbf{Q}_1)\mathbf{B}_{m-1}\right. \\ & & \left.+(\alpha_0 + \alpha_1\mathbf{Q}_1)\mathbf{C}_{m-1} + \mathbf{F}_{m-1}\right] \\ 0 & \mathbf{I}_{2,3} & 0 \\ 0 & 0 & I_{3,3} \end{bmatrix} \tag{48}$$

$$\mathbf{B}_{m-1,1} = [\mathbf{0}] \tag{49}$$

$$\mathbf{B}_{m-1,2} = \begin{bmatrix} \mathbf{I}_{3,3} & 0 & 0 \\ 0 & \mathbf{I}_{2,2} & 0 \\ -\Delta\psi\mathbf{I}_{3,3} & 0 & 0 \end{bmatrix} \tag{50}$$

and

$$\hat{\mathbf{g}}_{m-1,i} = \begin{Bmatrix} \Delta\psi\bar{\mathbf{g}}_{m-1} \\ 0 \\ 0 \end{Bmatrix} \tag{51}$$

Finally, matrices $\mathbf{Q}_1$ and $\mathbf{Q}_2$ are defined as

$$\mathbf{Q}_1 = \begin{bmatrix} 2 & 0 & 0 \\ 0 & 2 & 0 \\ 0 & 0 & \frac{4}{3} \end{bmatrix} \tag{52}$$

$$\mathbf{Q}_2 = \begin{bmatrix} -1 & 0 & 0 \\ 0 & -1 & 0 \\ 0 & 0 & -\frac{1}{3} \end{bmatrix} \tag{53}$$

The Local Truncation Error and Consistency

Let $\mathbf{F}(q)_i^j = 0$ represents the equation approximating of the given partial differential equation. It is assumed that $\mathbf{q}$ is the soluiotn of the finite difference equation and $\mathbf{u}$ is the exact solution of the partial differential equations (5-7) The value of $F(u)_i^j$ is called the local truncation error t_i^j at the (i,j) mesh point. $F(u)_i^j$ measures the amount of error by which values of the exact solution of the partial differential equation differs from the approximate numerical solution.

By using Taylor expansions, t_i^j can be easily expressed in terms of powers of $\Delta\bar{x}_i$, $\Delta\psi$ and the partial derivatives of q at $(\bar{x}_i, \psi_j)$. Although u and its derivatives are generally unknown, the analysis provides a method for comparing the local accuracies of different difference schemes approximating the partial differential equation. Then $\mathbf{F}_i^j(\mathbf{q})$

$$\mathbf{F}_i^j(\mathbf{q}) = \begin{Bmatrix} \frac{\mathbf{q}_{t_i}^{j+1} - \mathbf{q}_{t_i}^j}{\Delta\psi} - \bar{\mathbf{A}}_i^j \delta^2 \mathbf{q}_{m_i}^j - \bar{\mathbf{B}}_{d_i}^j \delta^2 \mathbf{q}_{d_i}^j - \bar{\mathbf{C}}_i^j \delta \mathbf{q}_{d_i}^j \\ -\bar{\mathbf{D}}_i^j \mathbf{q}_{t_i}^j - \bar{\mathbf{E}}_i^j \mathbf{q}_{m_i}^j - \bar{\mathbf{F}}_i^j \mathbf{q}_{d_i}^j - \bar{\mathbf{g}}_i^j \\ \frac{\mathbf{q}_{m_i}^{j+1} - \mathbf{q}_{m_i}^j}{\Delta\psi} - \mathbf{I}_{23} \delta^2 \mathbf{q}_{t_i}^{j+1} \\ \frac{\mathbf{q}_{d_i}^{j+1} - \mathbf{q}_{d_i}^j}{\Delta\psi} - \mathbf{I}_{33} \mathbf{q}_{t_i}^j \end{Bmatrix} = \mathbf{0} \tag{54}$$

The local truncation error vector due the approximate solution, $\mathbf{t}_i^j$ is

$$\mathbf{t}_i^j = \begin{Bmatrix} \frac{1}{2}\Delta\psi \mathbf{u}_d^{j^{**}} - \frac{1}{2}\Delta\bar{x}^2 [\bar{\mathbf{A}}_i^j \mathbf{u}_{m_i}^{j^{++++}} + \bar{\mathbf{B}}_i^j \mathbf{u}_{d_i}^{j^{++++}} + \frac{3}{4}\bar{\mathbf{C}}_{d_i}^{j^{+++}}] \\ \frac{1}{16}\Delta\psi \mathbf{u}_{m_i}^{j^{**}} - \mathbf{I}_{2,3} \left(\Delta\psi \mathbf{u}_{t_i}^{j^{*++}} + \frac{1}{2}\Delta\psi^2 \mathbf{u}_{t_i}^{j^{***++}} \right) \\ \frac{1}{2}\Delta\psi \mathbf{u}_{d_i}^{j^{**}} - \Delta\psi \mathbf{u}_{t_i}^{j^{**}} \end{Bmatrix} \tag{55}$$

Hence,

$$\mathbf{t}_i^j = O(\Delta\psi) + O(\Delta\bar{x}^2) \tag{56}$$

The principal part of the truncation error vector $\mathbf{t}_i^j$ shows that second order accuracy has been obtained for $\mathbf{u}_d, \mathbf{u}_t$ and $\mathbf{u}_m$ for spatial derivatives by central differencing. The accuracy for the time derivatives of displacements, velocities and defined variables $\mathbf{u}_m$ are still first order in time.

Consistency or Compatibility

It is possible to approximate a partial differential equation by a time-space, $\Delta\bar{x} - \Delta\psi$, grid work of elements which yields stable solutions. However, the resulting solution may converge to the solution of a different differential equation as the mesh lengths tend to zero. This approximate method is said to be inconsistent or incompatible.

For the exact solution u, the local truncation error is

$$t_i^j = F_i^j(\mathbf{u})$$

at a given node point $(\bar{x}_i, \psi_j)$. The difference equation is then consistent if the limiting value of each local truncation error tend to zero as $\Delta\bar{x} \to 0, \Delta\psi \to 0$. The principal local truncation error t_i^j, of the proposed numerical scheme tends to zero as the mesh lengths approches to zero and the consistency condition is satisfied [24].

Necessary and Sufficient Condition for Stability

The proposed numerical procedure,

$$\mathbf{q}^{G^{j+1}} = \check{\mathbf{A}}^{G^j}\mathbf{q}^{G^j} + \check{\mathbf{g}}^j \tag{57}$$

can also be written recursively as

$$\mathbf{q}^{G^{j+1}} = \check{\mathbf{A}}^{G^j}\check{\mathbf{A}}^{G^{j-1}}\ldots\check{\mathbf{A}}^{G^0}\mathbf{q}^{G^0} + \check{\mathbf{A}}^{G^j}\check{\mathbf{A}}^{G^{j-1}}\ldots\check{\mathbf{A}}^{G^1}\check{\mathbf{g}}^1 + \ldots + \check{\mathbf{A}}^{G^j}\check{\mathbf{g}}^{j-1} + \check{\mathbf{g}}^j \tag{58}$$

The numerical stability discussions requires that the largest eigenvalue of each matrices $\check{\mathbf{A}}^{G^j}$, i.e. the spectral radius $\rho(\check{\mathbf{A}}^{G^j})$ of $\check{\mathbf{A}}^{G^j}$ must satisfy [20,21,22,23]

$$\rho(\check{\mathbf{A}}^{G^j}) \leq 1 \tag{59}$$

in order to make the given numerical scheme is stable. Therefore, matrix $\check{\mathbf{A}}^{G^j}$ should be assembled and stability requirement (59) must be checked for each azimuthal step of the calculation.

Convergence

In order to prove that the approximate solution of the given partial differential equation is unique when it exists, convergence of the approximate equations must be also analyzed. As stated by Lax's Equivalence theorem [22] for a given properly posed initial problem and a finite difference approximation to it that satisfies the consistency condition, stability is the necessary and sufficient condition for convergence.

RESULTS AND DISCUSSIONS

In this section some numerical results are presented to illustrate the application of the approximate method to solve rotor blade aeroelastic equations. Since the objective of this paper is primarily to illustrate the application of the approximate method to find transient and steady-state response of rotor blade in hover and forward flight conditions, certain simplifications and assumptions are made as follows.

- A uniform inflow model is used for forward flight condition.
    1. For hover condition, advance ratio μ is set equal to zero and cyclic pitch components are neglected. A uniform inflow is assumed to be equal to its value at 0.75 span and written as

$$\lambda = \left(\frac{a}{\sigma}\right)\left[\left(\frac{1 + 24\,\theta}{a\sigma}\right)^{\frac{1}{2}} - 1\right]. \tag{60}$$

    2. For forward flight condition, inflow is assumed to be uniform along the blade and cyclic inflow components are set equal to zero. Uniform inflow λ_0 is written as

$$\lambda_0 = \mu\tan\alpha_v + \frac{C_T}{2(\mu^2 + \lambda_0)^{\frac{1}{2}}} \tag{61}$$

    The cyclic pitch variation for forward flight is calculated from

$$\theta = \theta_0 + \theta_{1S}\sin\psi + \theta_{1C}\cos\psi \tag{62}$$

    where all trim values for a given weight coefficient C_W are obtained from reference [18].

- Hub and tip loses are not included.
- A two dimensional, strip type, quasiateady aerodynamic model is used where Theodorsen lift deficiency function $C(k)$ is set equal to unity.
- Structural and mass properties of the blade are assumed to be uniform along the blade. All offsets from the elastic axis are also neglected.
- Reverse flow effects are not included.

Computational Details

For forward flight conditions, the approximate time-space finite element of the finite difference equations contain periodic coefficients. Transient and steady-state responses are obtained by spanwise and azimuthal marching. Expilict difference scheme does not require any matrix inversion process. For numerical stability analysis the spanwise global matrix $\bar{\mathbf{A}}^{G^j}$ is needed to be assembled at each azimuth step when the numerical stability is desired to check but its inverse is not required. The matrix $\bar{\mathbf{B}}^G$ in equation (38) is only function of spatial mesh distribution and its inverse is needed to be calculated once.

Throughout the entire analysis, uniform equal mesh size, $\Delta\bar{x}$ and azimuthal steps, $\Delta\psi$, are used. Spatial mesh size, $\Delta\bar{x}$, is only changed to analyze the effect of spatial discretization on the blade responses. Azimuthal step, $\Delta\psi$, is changed to obtain faster azimuthal marching with in the limits of numerical stability condition for a fixed mesh size, $\Delta\bar{x}$, for given blade and flight condition parameters.

Numerical Stability and Convergence Results

For a given mesh size and system parameters, numerical stability analyses are performed and the maximum azimuthal step, $\Delta\psi$, are determined. of integration. The highest azimuthal step is the one that satisfies the numerical stability condition

$$\rho(\bar{\mathbf{A}}^{G^j}) \leq 1.$$

Result for numerical stability anayses are given in in Table 2 where maximum azimuthal steps, $\Delta\psi_{max}$, are given for different mesh sizes for stiff inplane blade. Analyses are carried out for advance ratios, $\mu = 0.2$ and $\mu = 0.4$, but the difference between two sets of result is insignificant. A similar analysis is also performed for stiff inplane configuration and results are given in Table 2. In Figure (3), effects of spatial mesh sizes on flap-lag-torsion responses are illustrated. Different tip responses are plotted for $\Delta\bar{x} = 0.2,\ 0.1,$ and 0.05, respectively. Convergence in peak to peak values of tip deflections are observed as the mesh size decreased.

Results for Forward Flight Conditions

Results for forward flight conditions are presented in this section. Primarily two different blades, soft and stiff inplane, are considered. Rotor blade parameters are given in Table 3. For a given blade, forward flight parameters and a choosen spatial mesh size, $\Delta\bar{x}$, numerical stability analysis is performed and the highest azimuthal step, $\Delta\psi_{max}$, consistent with limits of numerical stability is obtained.

Solutions for forward flight are initiated by all zero initial conditions first for hover condition by setting advance ratio equal to zero. The pitch setting for hover, θ_C, is also set equal to the steady pitch component, $\theta_C = \theta_0$, obtained by propulsive trim analysis for the desired forward flight conditions. During the hovering period, a uniform inflow assumed to be equal to its value at 0.75 span, given by equation (60), is used.

Flight condition is switched from hovering to forward flight by introducing the cyclic pitch componenets to the corresponding pitch variation by a linear incremental procedure until their trim solution values are reached. Increments for the cyclic pitch components are introduced such that during this switching period, at j^{th} azimuthal step, the cyclic pitch components are taken as

$$\theta_{1C}^{j+1} = \theta_{1C}^{j} + \Delta\theta_{1C} \tag{63}$$

$$\theta_{1S}^{j+1} = \theta_{1S}^{j} + \Delta\theta_{1S} \tag{64}$$

where

$$\Delta\theta_{1C} = \frac{\theta_{1C}}{N_{sw}} \tag{65}$$

μ	λ_0	α_v	θ_0	θ_{1S}	θ_{1C}
0.2	-.02040	.0406	.1060	-.0465	.0110

Table 1: Propulsive Trim Values, Uniform Inflow, $C_W = .005$, [18]

$\Delta\psi_{max}$	$\Delta\bar{x} = 0.2$	$\Delta\bar{x} = 0.125$	$\Delta\bar{x} = 0.10$	$\Delta\bar{x} = 0.05$
Soft inplane	.1750	.0325	.0100	.0050
Stiff inplane	.0875	.0150	.0075	.0025

Table 2: Maximum allowable time intervals for different mesh sizes.

$$\Delta\theta_{1S} = \frac{\theta_{1S}}{N_{sw}} \tag{66}$$

Then the cyclic pitch variation at $(j+1)^{th}$ azimuth step during this switching period is calculated as

$$\theta^{j+1} = \theta_0 + \theta_{1S}^{j+1} \sin\psi_{j+1} + \theta_{1C}^{j+1} \cos\psi_{j+1} \tag{67}$$

In above expression θ_{1C} and θ_{1S} are the cyclic pitch components obtained by trim solution and N_{sw} is the number of the azimuthal steps of this switching period. The advance ratio, μ, and the uniform inflow, λ_0, are set to their trim state values immediately at the beginning of switching state. Propulsive trim state values are obtain from reference [18]. For weight cofficient, $C_W = .005$ and advance ratio, μ =0.2, trim states are given in Table 1.

Results for Flap-Lag-Torsion Dynamics in Forward Flight

The proposed time-space finite element procedure based on finite difference approximations used to solve rotor blade partial equations with flap-lag-torsion motions. Rotor blade equations, given by Taylor [18] are solved for different blade parameters and flight conditions. Highest azimuthal step, $\Delta\psi_{max}$, is obtained by the numerical stability analysis, including only flap-lag motions for the same parameters, is used for solving the governing equations with flap-lag-torsion motions. The cyclic pitch values are introduced by a linear incremental procedure as explained in previous section.

A typical transient and steady-state responses with flap-lag-torsion motions is presented in Figure 2. Corresponding blade parameters are given in Table 3 and advance ratio is set equal to $\mu = 0.2$. For this particular case, two different switching time intervals, $\Delta\psi_{sw} = N_{sw}\Delta\psi$, are used. As seen from Figure 2, for the longer switching period, $\Delta\psi_{sw}$=3.0 *rad*, lag transients alternated in less time for the case, $\Delta\psi_{sw}$=1.2 *rad*.

Steady-state tip responses of a soft inplane blade with flap-lag-torsion motions are obtained by solving the rotor blade partial differential equations given by Taylor [18]. Results for soft inplane rotor with advance ratio, $\mu = 0.2$ are compared with results of Reference [18] and presented in Figure 3. As illustrated from Figure 3, flap-lag-torsion tip deflections obtained by explicit finite difference method show good agreements with results of Taylor [18] where Galerkin method has been used for spatial discretization and temporal dependency is eliminated by harmonic balance technique. Percentages of differences between two sets of results are between %9 and %2 where the highest difference is observed in between flap tip responses.

A similar analysis is also made for stiff inplane configuration with advance ratio, μ=0.2. Figure 4 illustrates the results obtained by the use of finite difference method and results of reference [18]. Similar with the previous case, good agreements are obtained for steady-state flap, lag and torsion tip responses. In this case, flap tip deflection results differed with %6 and differences in between two sets of results for flap,lag and torsion motions are %3.5 and %4 respectively. For the stiff inplane configuration only the inplane stiffness is different from the soft inplane configuration where $\bar{\omega}_{L1}$ =1.417 for stiff blade. All the other parameters are given in Table 3. Sample phase plots are also plotted for several blade revolutions to

First rotating lag frequency :	$\bar{\omega}_{L1}$ =0.732 (soft) (Λ_2=.01079)
	$\bar{\omega}_{L1}$ =1.417 (stiff) (Λ_2=.14745)
First rotating flap frequency :	$\bar{\omega}_{F1}$ =1.125 (Λ_1 =.01079)
First rotating torsion frequency :	$\bar{\omega}_{\phi 1}$ =3.176 ($\vec{GJ}$=.00203)
	$\left(\frac{k_A}{k_M}\right)^2 = 1.0$
	$\left(\frac{k_M}{R}\right) = .025$
	$\left(\frac{k_{m_1}}{k_{m_2}}\right) = 0.0$
Semicord :	$\frac{b}{R}$=0.0275
Drag coefficient :	D_{D0}=0.01
Solidity ratio :	σ=0.07
Lock number :	ν=5.5
2-D Lift curve slope :	$a = 2\pi$
Weight coefficient :	C_W=0.005
Aerodynamic center offset :	X_A=0.0
Precone angle :	β_p=0.0
Advance ratio :	μ=0.2

Table 3: Configuration Parameters for Flap-Lag-Torsion Motions in Forward Flight

illustrate that blade resposes had reached to their steady-state. In Figure 5, the effect of nonlinear terms on blade tip responses are illustrated for different stiff inplane configuration for advance ratio μ=0.2. As also see from the Figure 5, nonlinear terms have significant effect on flap and torsion tip responses for the stiff inplane configuration.

CONCLUSIONS AND REMARKS

In view of the results of present study the following conclusions can be drawn.

- Azimuthal time step, $\Delta\psi$, is found to be the key parameter in azimuthal marching calculations by the present conditionally stable explicit scheme. Highest azimuthal step, $\Delta\psi$, obtained by numerical stability analysis, is dependent mainly on the spatial discretization, the mesh size $\Delta\bar{x}$, and the inplane bending stiffness Λ_2 which is as blade structural parameter. Smaller mesh sizes required smaller azimuthal steps. As the inplane bending stiffness is increased, the numerical stability condition is satisfied by smaller azimuthal steps as compared to the azimuthal steps for the blades with softer inplane stiffnesses.

- Switching period from hover to forward flight conditions has an important effect on transient response of the blade. Although the advance ratio, μ, and the inflow coefficient, λ, are set equal to their trim values at the beginning of this period, introducing the cyclic pitch components in an incremental manner eliminated very sharp transient responses. Besides, longer switching periods helped the transients die out quicker.

- It is observed that the blade inplane stiffness, Λ_2 and the advance ratio, μ, have a significant effect on the transient response of the rotor blade. In general, lag motions reach their steady-state values after longer transient periods than flap-lag motions. For higher inplane stiffnesses and advance ratios, transients also died out quicker than for soft inplane blade configurations and low advance ratios.

- Size of the spatial mesh discretization, $\Delta\bar{x}$, has an important effect on the blade responses, especially on torsion. As the spatial mesh size increases, the peak-to-peak values of the blade responses also increase but for values of $\Delta\bar{x} \geq 0.1$ blade responses show a convergent behavior.

- This explicit time-space finite element approach based on finite difference procedure does not require inversion of large matrices and can be extended to study more complicated problems such as gust response, nonuniform and bearingless rotor blades. A benefit of this approach is that accuracy and convergence can be assured and a suitable scheme can be selected for the needed application.

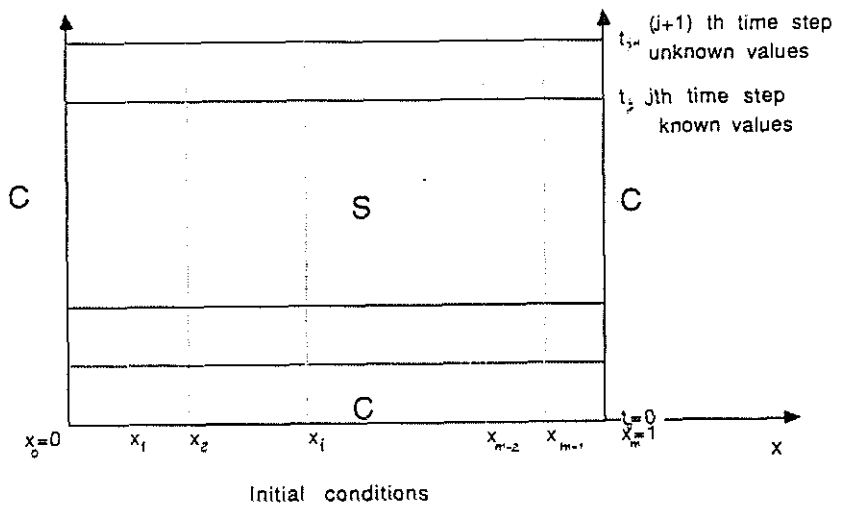

Figure 1: Spatial and Azimuthal Mesh Distributions of Rectangular Time-Space Grid Work

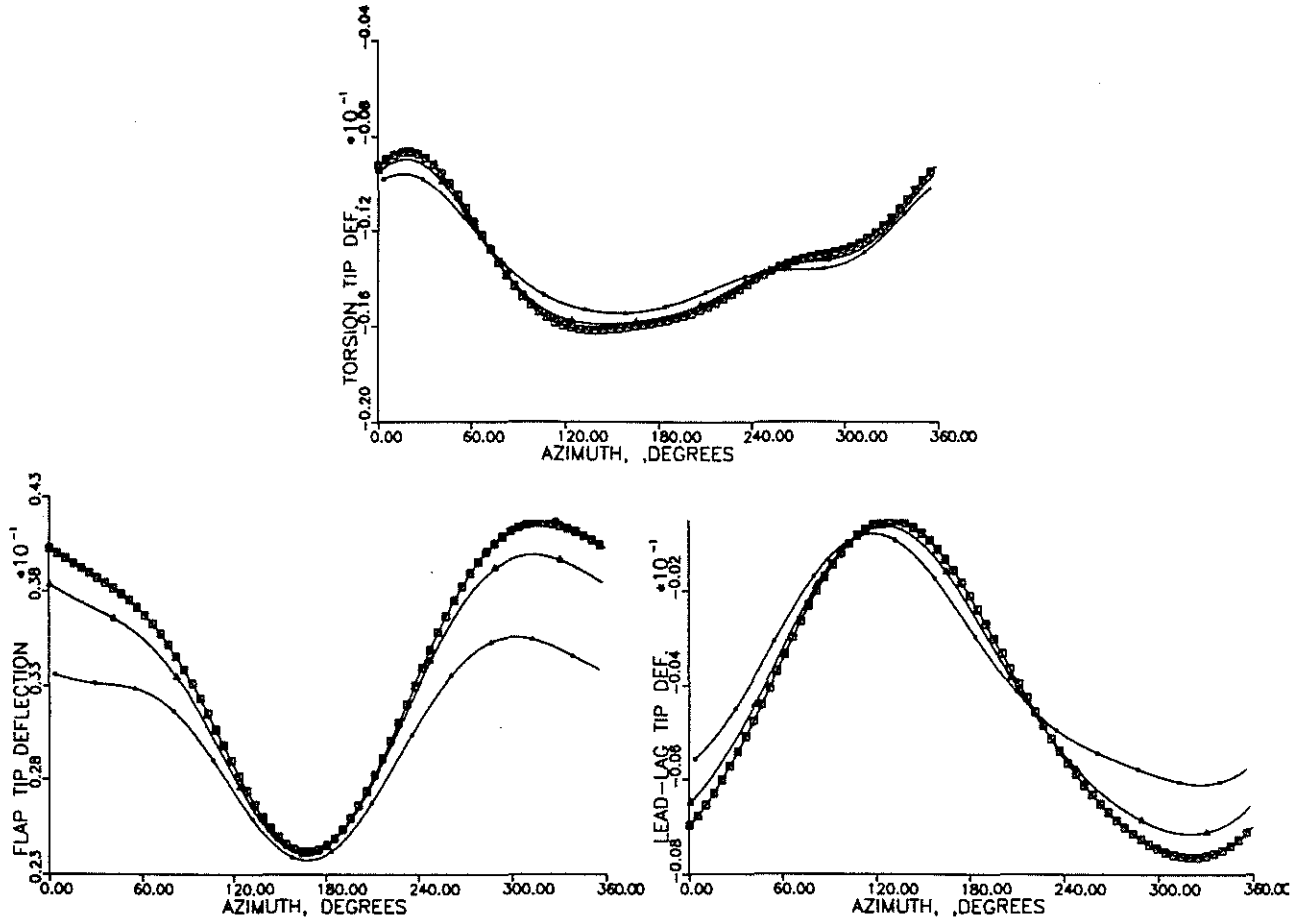

□ $\Delta\bar{x} = 0.05$, △ $\Delta\bar{x} = 0.1$, • $\Delta\bar{x} = 0.2$

Figure 2: Numerical Convergence: Effect of Mesh Sizes on Blade Response in Forward Flight, $\mu = 0.2$, Stiff Inplane

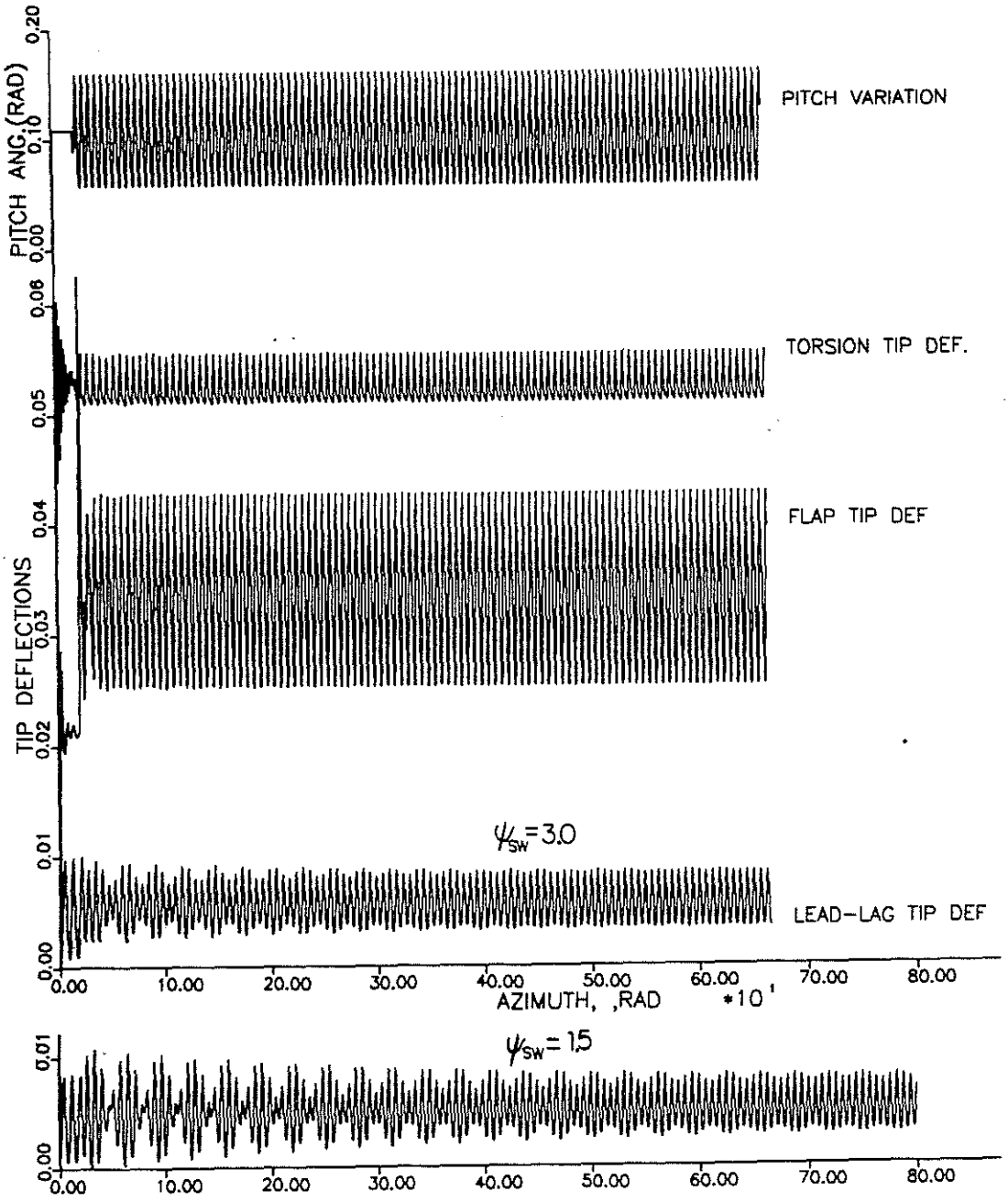

Figure 3: Transient and Steady State Responses in Forward Flight, $\mu = 0.2$, Soft Inplane

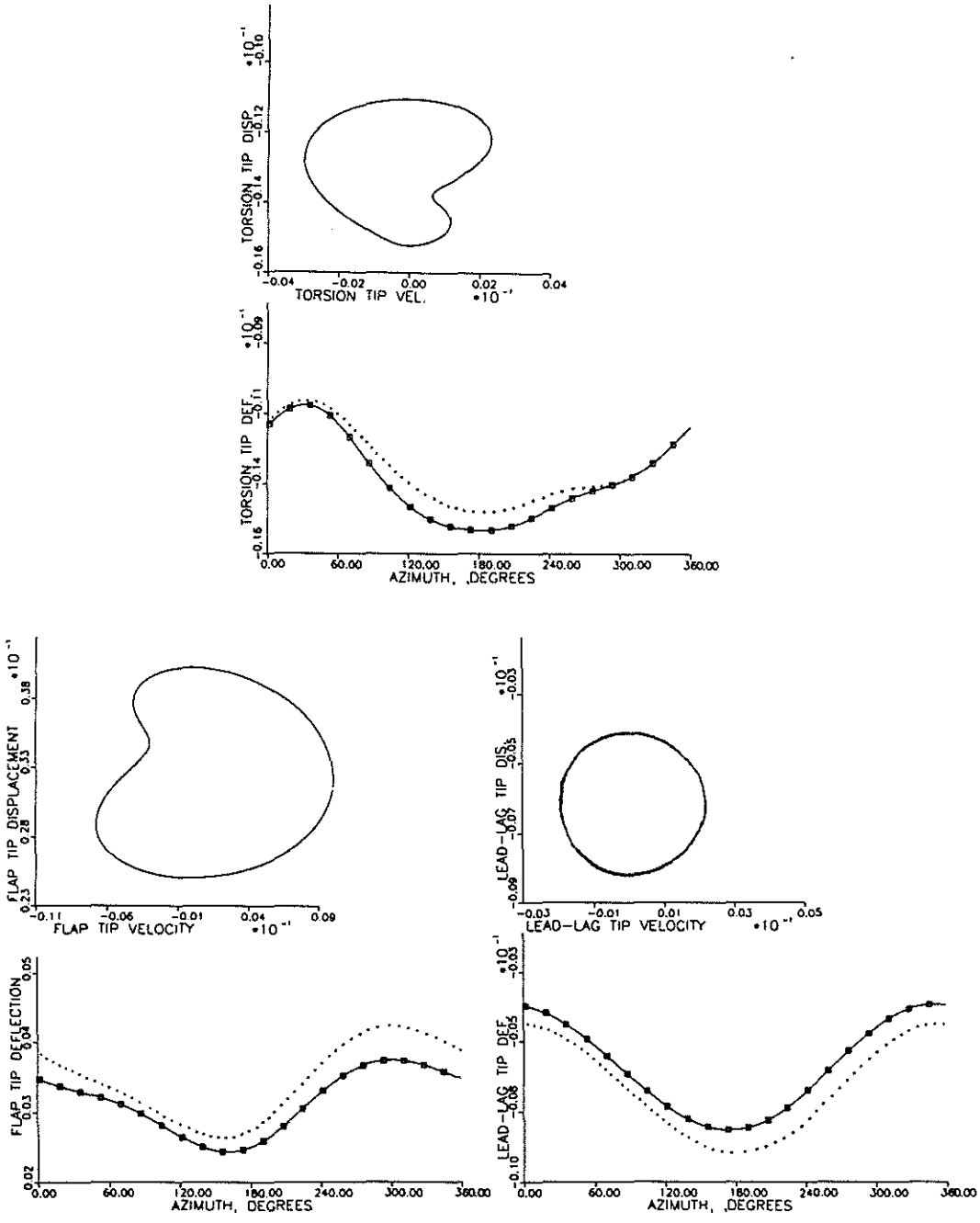

□ Present, • Reference [18]

Figure 4: Verification: Flap-Lag-Torsion Responses in Forward Flight, $\mu = 0.2$, $\beta_{pc} = 0.0$, Soft Inplane

References

[1] Jonnalagadda, V.R.P. , " A Derivation of Rotor Blade Equations of Motion in Forward Flight and Their Solutions " Doctoral Dissertation, Scholl of Aerospace Engineering, Georgia Institute of Technology, Atlanta Georgia, August, 1985.

[2] Hodges, D.H. and Ormiston, R.A., " Nonlinear equations for bending of ro- tating beams with application to linear flap-lag stability of hingeless rotors ", NASA TM X-2770 (1973).

[3] Karunamoorthy, S.N. and D.A. Peters, " Use of Hierarchial Elastic Blade Equations and Automatic Trim for Rotor Response ", Vertica Vol. 11, No. 1/2, pp. 233-248, 1987.

[4] Straub, F.K. and P.P. Friedmann, " Application of the Finite Element Met- hod to Rotary Wing Aeroelasticity ", NACA CR 165854, Feb. 1982.

[5] Sivaneri, N.T., and I. Chopra, " Dynamic Stability of a Rotor Blade Using Finite Element Analysis " AIAA Journal, Vol. 20, No. 5, pp.716-723, May 1982.

[6] Bir, S.G. and I. Chopra, " Gust Response of Hingeless Rotors ", Journal of AHS, Vol. 31, No. 2, pp. 33-46, April 1986.

[7] Bir, S.G. and I. Chopra, " Prediction of Blade Stresses Due to Gust Loading", Vertica , Vol. 10, No. 314, pp.353-361, 1987.

[8] Friedmann, P.P, Recent Trends in Rotary-Wing Aeroelasticity, Vertica, Vol. 11, No. 12, pp. 139-170. 1987.

[9] Panda, D. and I. Chopra, " Flap-Lag-Torsion Stability in Forward Flight ", Journal of AHS Vol. 30, No. 4, Oct. 1985.

[10] Dugundji, J., and H. Wendell, " Some Analysis Methods for Rotating Systems with Periodic Coefficients ", AIAA Journal, Vol. 21, No. 6, pp. 890-897, June 1983.

[11] Borri, M., " Helicopter Dynamics by Finite Element Time Approximaton ", Computers andMathematics Applications, Vol 12 A, pp.149-160, 1986.

[12] Panda, B., and I. Chopra, " Dynamics of Composite Rotor Blades in Forward Flight", Vertica, Vol. 11, No. 112, pp. 187- 209, 1987.

[13] Izadpanah, A.P., "p-Version Finite Element for the Space-Time Application to Floquet Theory", Doctoral Dissertation, School of Aerospace Engineering, Georgia Institute of Technology, Atlanta, Georgia, August 1986.

[14] Ritchmeyer, R.D., and K.W. Morton, *Difference Methods for Initial-Value Problems*. Interscience Publisher, Second Edition, John Wiley and Sons, Inc., 1967.

[15] Gladwell, I., and R. Wait, *A Survey of Numerical Methods for Partial Differential Equations*, Clarendon Press, Oxford 1979.

[16] Abhyankar, N.S. , " Studies in Nonlinear Structural Dynamics: Chaotic Behavior and Poyntic Effects," Doctoral Dissertation, School of Aerospace Engineering, Georgia Institute of Technology, Atlanta, Georgia, August 1986.

[17] Panda, B., " Dynamic Stability of Hingeless and Bearingless Rotors in Forward Flight ", Computers and Mathematics with Applications, Vol. 12A, No. 1, pp. 111- 130, 1986.

[18] Taylor, D. J., "A Method for the Efficient Calculation of Elastic Rotor Blade Dynamic Response in Forward Flight ", Doctoral Dissertation, School of Aerospace Engineering, Georgia Institute of Technology, Atlanta, Georgia, March 1987.

[19] Kottapalli, S.B.R.; Friedmann, P.P. and Rosen, A., " Aeroelastic Stability and Responce of Horizantal Axis Wind Turbine Blades ", AIAA Journal, Vol. 17, pp. 1381-1389, 1979.

[20] Wait, R., and A.R. Mitchell, *Finite Element Analysis and Applications*, pp. 159- 162, John Wiley and Sons, Great Britain, 1985.

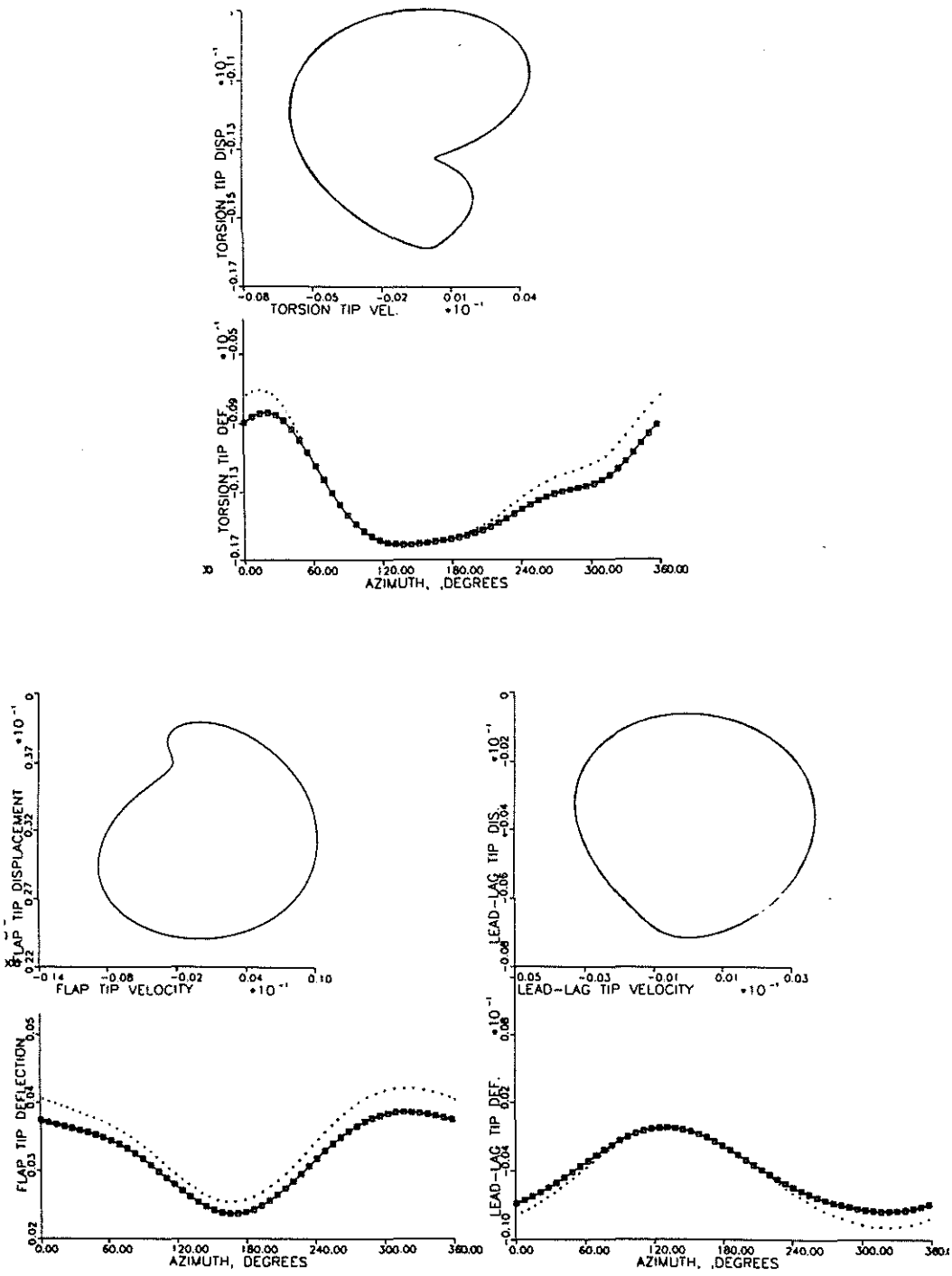

□ Present, • Reference [18]

Figure 5: Verification: Flap-Lag-Torsion Responses in Forward Flight, $\mu = 0.2$, β_{pc} =0.0, Stiff Inplane

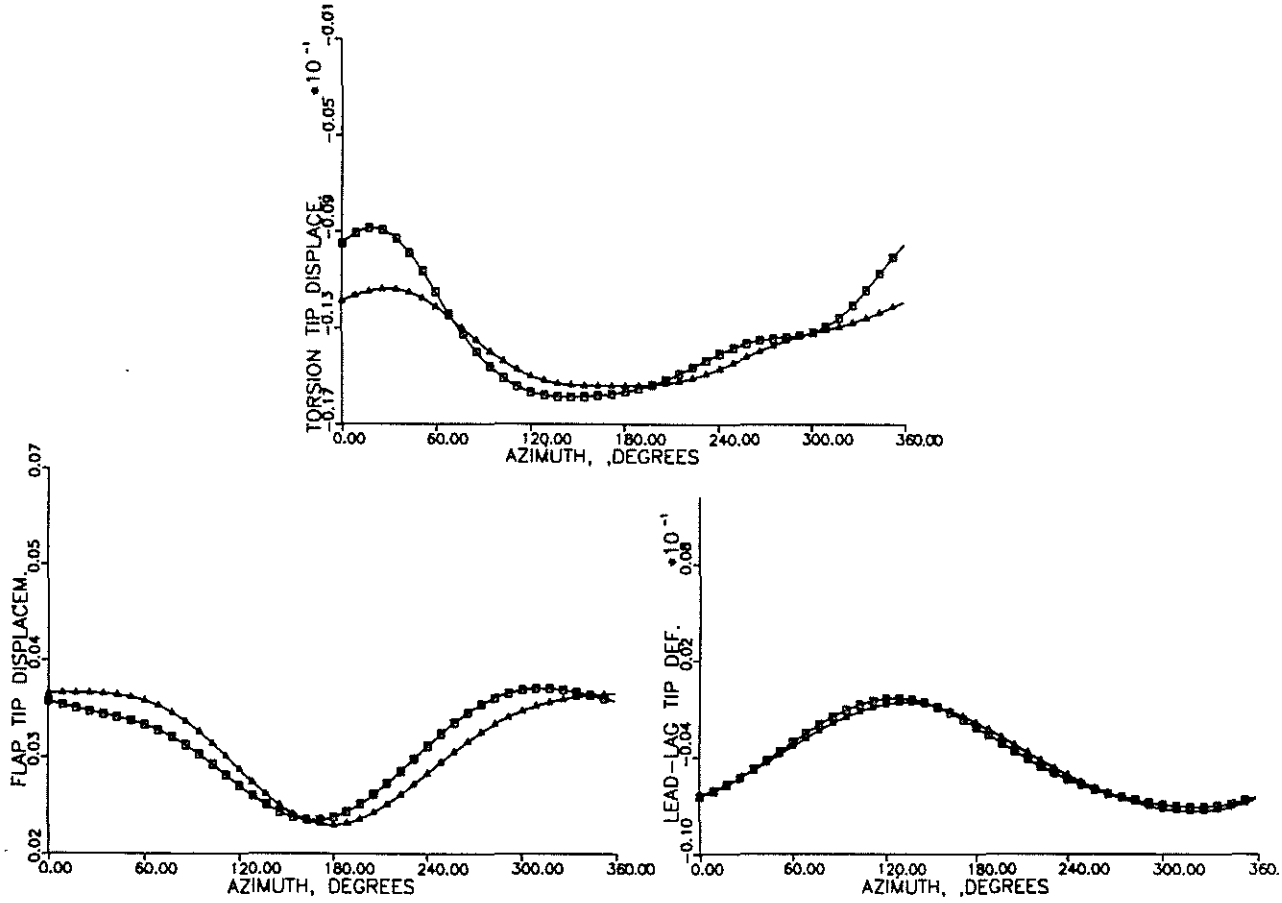

Figure 6: Effect of Nonlinear Terms on Blade Responses, Stiff Inplane, $\mu = 0.2$, $\beta_{pc} = 0.0$, $\square$ = Nonlinear, $\triangle$ = Linear

[21] Mitchell, A.R. and D.F. Griffiths, *The Finite Difference Method In Partial Differential Equations*, pp. 38-43, John Wiley and Sons , Great Britain, 1980.

[22] Ritchmyer, R. D., and Morton, K. W., *Difference Methods for Initial-Value Problems*, 2nd Edition, Intersciece-Wiley, 1967.

[23] Smith, G.D., *Numerical Solution of Partial Differential Equations: Finite Difference Methods*. Oxford Applied Mathematical and Computing Science Series, Claredon Press, Oxford, 1985 (third edition).

[24] Yillikci, Y.K., "Finite Difference Techniques and Rotor Blade Aeroelastic Partial Differential Equations with Quasisteady Aerodynamics ", Doctoral Dissertation, School of Aerospace Engineering, Georgia Institute of Technology, Atlanta, Georgia, December 1989.